Electron Fringes on a Quantum Wedge

I. B. Altfeder,[1] K. A. Matveev,[1,2] and D. M. Chen[1]

[1]*The Rowland Institute for Science, Cambridge, Massachusetts 02142*
[2]*Department of Physics, Duke University, Durham, North Carolina 27708-0305*
(Received 11 October 1996)

Using molecular beam epitaxy we have fabricated a quantum wedge: a nanoscale flat-top lead island on a stepped Si(111) surface. Imaging the top surface of the wedge with a scanning tunneling microscopy reveals the phenomenon of electron interference fringes: a discrete periodic spatial variation of the tunnel current originating from the quantization of electron states in the wedge. [S0031-9007(97)02817-2]

Fizeau fringes, a well known interference phenomenon, occur when a monochromatic light illuminates a thin optical wedge [1]. Because of the wave nature of electron a similar phenomenon of electron interference fringes also exists, and has been observed by transmitting an energetic coherent electron beam through a thin film [2]. Unlike the optical interference, electron fringes can in principle appear spontaneously on a thin metal wedge, since the interfering particles, electrons, are already present in the metal and confined by the boundaries [3]. Observing these fringes, however, requires a technique capable of imaging a standing wave inside a wedge. A perfect tool for this task is a scanning tunneling microscope (STM), which probes the weak evanescent tails of electrons outside the metal without destroying the interference pattern. Indeed, the STM has been used successfully to reveal the interference phenomena due to the scattering of electrons in a vacuum gap [4,5], at surface defects [6,7], or in a quantum corral [8].

To achieve sharp interference fringes, one can exploit the strong energy quantization of the electron states in a metal wedge with an average thickness of a few nanometers. We name a nanoscale wedge with its thickness varied monotonically by discrete atomic planes a *quantum wedge,* for a change of its thickness by a single atomic plane can lead to an appreciable shift of the electron energy spectrum. The discrete nature of a quantum wedge can give rise to a discrete contrast in the interference pattern. For example, for a metal with a Fermi electron wavelength $\lambda_F = 4a_0$ (a_0 being the atomic plane spacing), the variation in the thickness by a_0 changes the interference condition from destructive to constructive, or *vice versa,* and the fringe contrast will have a square wave profile. In this Letter we demonstrate the first experimental realization of such electron interference fringes on a quantum wedge. The quantum wedge was fabricated by the epitaxial growth of Pb on a stepped surface of Si(111), while the fringes were observed *in situ* with a low-temperature STM.

It has been previously shown that on the Si(111) surface three-dimensional islands of Pb begin to form after an initial growth of 2–3 wetting layers, and the growth planes are the Pb(111) planes [9,10]. The Fermi wavelength of Pb along the [111] direction has been determined to be $\lambda_F = 3.7a_0$ ($a_0 = 2.86$ Å) [11]. The small deviation of the λ_F from the ideal value of $4a_0$ implies that the twofold periodic interference pattern up to 12 fringes can be formed. These properties make Pb an excellent material for the quantum wedge.

The experiment was performed in an ultrahigh vacuum system with a base pressure of 3×10^{-11} Torr. It is equipped with standard tools for substrate preparation, surface analysis, and molecular beam epitaxy, and with a STM operating in the temperature range between 4.8 and 300 K. The Si(111) substrate was cleaned by a sequence of Ar ion etching and dc current heating to 1000 °C. Pb was deposited from an effusion cell with the Si substrate being held near 0 °C. The quality of the Si substrate and the Pb deposition was checked by Auger spectroscopy and reflective high energy electron diffraction (RHEED) and both were free of impurities and exhibited high crystallinity. The STM measurements were performed at 4.8 and 77 K, and yielded essentially the same results.

Figures 1(a) and 1(b) are two typical STM images of a Pb island on Si(111) obtained with opposite tip biases at 4.8 K. The topography of the Pb layer surrounding the island shows that the monatomic steps on the Si(111) substrate are separated by 100–1000 Å. The scan shown in Fig. 1(a) was performed at −5 V tip bias. It shows that despite the stepped substrate the top surface of the Pb island is atomically flat, so that on every successive Si terrace the thickness of the Pb island changes by one layer. Slope visible in the cross section of the island [Fig. 1(c)], and shallow steps of ~0.25 Å height aligned with the underlying Si steps [Fig. 1(a)], result from the misfit between the lattice spacing of Si (3.13 Å) and Pb (2.86 Å) in the [111] direction. The typical average thickness of the Pb wedge in our experiments is between 20 and 100 Å. Thus we conclude that these Pb islands grown on the stepped surface of Si(111) possess the geometry of a quantum wedge.
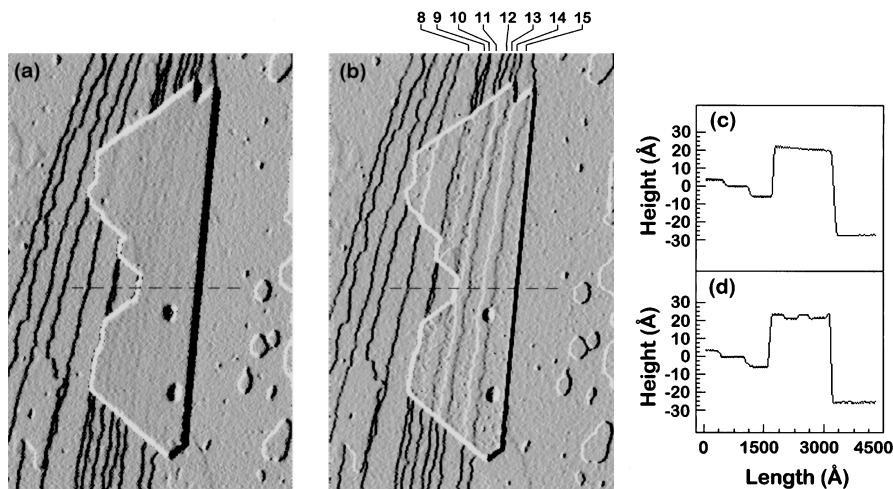
FIG. 1.   (a) 7300 × 11 000 Å STM image taken with a tip bias of −5 V, showing a topography of the Pb wedge grown on a stepped Si(111) substrate. (b) STM image of the same wedge obtained with +5 V tip bias, showing the electron fringes on the surface of the wedge. Both images are differentiated with respect to the horizontal axis to enhance the step edges. (c),(d) Cross sections taken, respectively, from the originals of (a) and (b) as marked by the dashed lines.

In contrast, the STM image obtained at +5 V tip bias and its cross section [Figs. 1(b) and 1(d)] show that the top of the island is a sequence of up-and-down bands placed directly above the individual terraces of the substrate. The step height between the lower and upper bands varies from 0.5 to 1.0 Å. Comparison of Figs. 1(a) and 1(b) indicates that the observed up-and-down bands are not related to the surface morphology of the wedge, rather they reflect the change of the tunnel current with respect to the thickness of the wedge. Similar STM images were obtained with a tip bias from +1 to +8 V and at −1 V. As we will show, *these bands are the interference fringes of the electrons confined within the wedge,* as illustrated schematically in Fig. 2.

To verify the nature of the fringes, we have measured the tunnel *I-V* characteristics with the tip placed over different bands of the wedge at the same distance from the surface. A sequence of the *I-V* spectra is shown in Fig. 3 where the *number* corresponds to the same numbered band in Fig. 1(b). It indicates the *number* of Pb layers of the wedge under that particular band measured with

respect to the top of the wetting layers. The spectra reveal sharp steps with a separation Δ, which decreases from 1.4 to 0.7 eV as the thickness of the wedge increases. We observe a linear dependence between the inverse of Δ
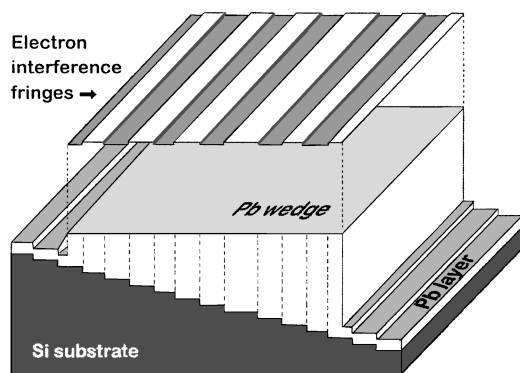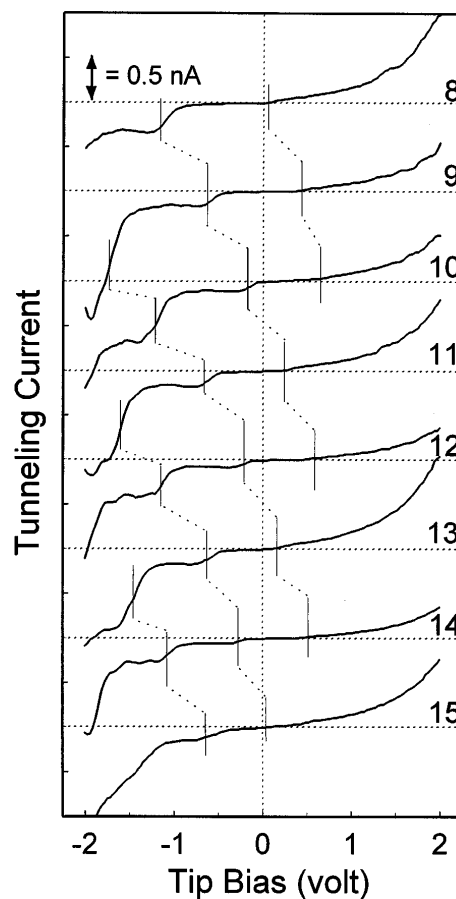

FIG. 2.   Schematic of a quantum wedge on a stepped substrate. Electron interference fringes are shown above the wedge. Vertical scale is enlarged by a factor of 100.

FIG. 3.   A series of *I-V* spectra measured at 4.8 K over different numbered bands on the surface of the Pb wedge shown in Fig. 1(b). Progression of the quantized steps is marked.

and the thickness of the wedge H, as clearly shown in Fig. 4. Tunnel spectra for the odd and even numbered bands are different, and the shift between the steps of two neighboring bands is approximately $\Delta/2$.

Because of the interference of electrons confined in the wedge, the total phase change $2Hk$ after an electron bounces off the two boundaries must be an integer in units of 2π, with k being the electron wave vector normal to the boundaries. Hence the allowed values of k are separated by π/H. For the electrons near the Fermi level the energy separation between such states is

$$\Delta = \pi \hbar \nu_F / H, \tag{1}$$

where $\hbar$ is Plank's constant, and ν_F is the Fermi velocity. From Fig. 4 and Eq. (1) we find ν_F along the [111] direction of Pb to be 1.9×10^8 cm/sec, in a good agreement with the value measured for the hole Fermi surface of Pb [3,11]. When the number of layers N is small its relation with the thickness H is nontrivial. Within the tight-binding model one finds $H = (N + 1)a_0$. The extrapolated $1/\Delta$ crosses the H axis at a negative value, implying that the actual thickness of the wedge needs to be increased by 2 to account for the wetting Pb layers. Interestingly, *the tunnel spectroscopy can be used to determine the number of Pb wetting layers.*

Strong quantization of electrons also leads to an appreciable shift of their energy spectra as the number of layers in the Pb wedge varies. For the states near Fermi level, the shift due to the change of thickness by one atomic plane is given by [12]

$$\delta = \frac{2a_0}{\lambda_F} \Delta, \tag{2}$$

and from the measured shift in Fig. 3 one finds $\lambda_F \approx 4a_0$, indicating a nearly half-filled Pb conduction band along the [111] direction as expected. To summarize, *the observed features in the I-V curves are a clear manifestation of the quantization of electron states in the Pb wedge.*

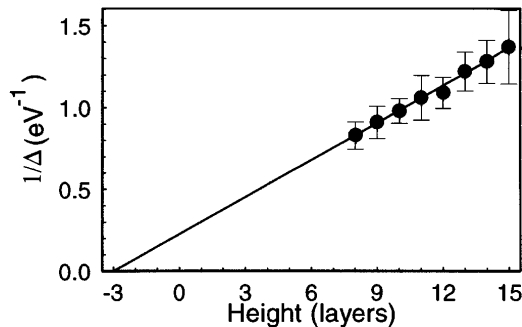To see how the quantization of electron states affects STM images we now address yet another important feature in the I-V curves. In Fig. 3, the tunnel current at a large positive tip bias oscillates between odd and even bands. An addition of just one Pb layer, i.e., a 10% variation of the height, changes the current by a factor of 2 or 3. Remarkably, this trend is interrupted between curves 9 and 10, as expected from the incommensurability between the λ_F and a_0 [a corresponding break in the fringe pattern at band 9 is also visible in Fig. 1(b)]. On the I-V curves at the positive tip bias only the step near zero bias is resolved. This step is associated with the highest occupied quantum state (HOQS). We notice that the closer the HOQS is to the Fermi level, the faster the tunnel current rises at higher biases.

To elucidate the asymmetry in the I-V characteristics with respect to the bias polarity, consider a simple model with a tunnel barrier of trapezoidal shape (see the insets in Fig. 5), and assume that the tunneling is allowed only for a set of discrete quantum states (QS) with momenta perpendicular to the surface of the wedge. Neglecting the small difference between the work functions ϕ of the Pb wedge and the tungsten tip, the tunnel current is expressed as

$$I(V) = \pm A \sum_i \exp$$
$$\times \left\{ -\frac{2}{\hbar} \int_0^d \mathrm{Re}\left[\sqrt{2m\left(\phi - E_i + \frac{x}{d} eV \right)} \right] dx \right\}, \tag{3}$$

where $\pm$ is a polarity of the bias, A a constant, m a free electron mass, e the charge of an electron, E_i the energy of the ith QS measured from the Fermi level, and d the width of the tunnel barrier. The sum is taken over the QS with energies E_i between 0 and $-eV$. Figure 5(a) shows
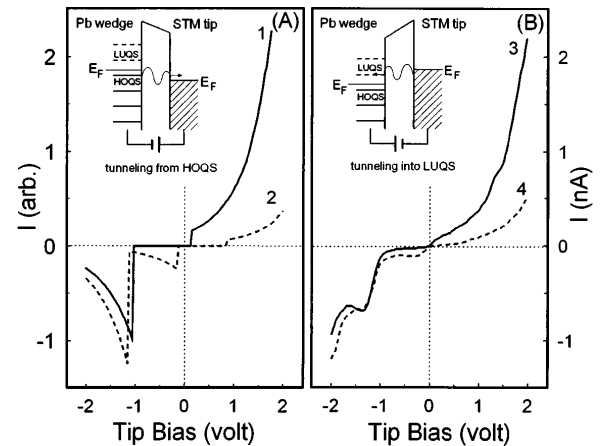

FIG. 4. Inverse of the separation between steps on the I-V curves in Fig. 3 as a function of the thickness of the wedge, measured in number of layers with respect to the Pb wetting layer surrounding the island.

FIG. 5. (a) Tunnel I-V curves calculated from Eq. (3) for two different electron energy spectra: the nearest state from the Fermi level is the *highest occupied quantum state* (curve 1) and the *lowest unoccupied quantum state* (curve 2). The parameters are $d = 10$ Å, $\phi = 4.0 eV$, $\Delta = 1.2 eV$ (for curve 1 and $1.0 eV$ for curve 2). (b) Corresponding experimentally measured I-V curves. Insets of (a) and (b): schematic of the barrier for the tunneling from HOQS and into LUQS, respectively.

the curves calculated from Eq. (3) for two energy spectra: the nearest state from the Fermi level is the HOQS (curve 1) or lowest unoccupied quantum state (LUQS) (curve 2). Two experimentally measured I-V curves (curves 3 and 4) are shown in Fig. 5(b) for comparison. We see that the one-dimensional model is in good qualitative agreement with the main features observed in the experiment. We attribute this to the focusing of the tunneling electrons in a vacuum gap [3], and to the nearly flat geometry of the hole Fermi surface of Pb around the [111] symmetry point [13].

The origin of the asymmetry of the I-V spectra lies in the fact that tunneling into the unoccupied QS involves a smaller barrier than tunneling from the occupied QS, as illustrated in the insets of Fig. 5. Each new step appears in the I-V curve when the Fermi level of the tip crosses a QS in the wedge. When the Fermi level of the tip sweeps from higher occupied QS towards lower unoccupied QS, the tunnel barrier increases for each new state, and the height of the steps in the I-V curve decreases. Between two neighboring steps on the I-V curve both the number and energies of the QS contributing to the tunnel current remains unchanged, whereas the energies of the participating states in the tip rise. As a result, after the step we see a region of increasing current. For unoccupied QS this gives rise to a negative differential conductance, as observed in our experiments [see Fig. 5(b)]. In the positive tip bias region, the dominant contribution to the current comes from the HOQS, because the tunnel barrier for this state is lower than for other occupied states. For the HOQS, the tunnel barrier is further reduced when this state levels closer to the Fermi level of the wedge. This results in the strong correlation between the position of the first I-V step at small positive bias and the current at large positive bias. On the other hand, at a large negative tip bias the QS just below the Fermi level of the *tip* is the primary source of the tunnel current. These states are near the top of the Pb conduction band, and their energy separation is estimated to be an order of magnitude smaller than Δ [11]. Therefore, the height of the tunnel barrier and hence the current do not change significantly between alternating bands.

These tunneling characteristics play a crucial role in the detection of the interference fringes from the quantized electrons in the wedge. Since the HOQS gives the principal contribution to almost the entire I-V spectrum at the positive tip bias, we in effect have a "monochromatic" source of electrons. We recall that it is the electrons with a wavelength close to λ_F that produce an abrupt transition from destructive to constructive interference with the

addition of each atomic plane in the wedge. The large oscillations of the tunnel current at high positive bias on alternating bands of the wedge provide the mechanism for the fringe contrast enhancement embodied in the tunnel junction. Hence we have chosen to demonstrate these fringes at a relatively large bias of $+5$ V [Fig. 1(b)], though they can be observed at other biases or in a differential conductance mode. At the other extreme, at large negative tip bias the contrast is diminished, and we are able to unveil the surface morphology of the quantum wedge at the same time.

In conclusion, we have successfully demonstrated a quantum mechanical analog of the classical optical wedge experiment. By constructing a metallic quantum wedge, we are able to create and detect the spatial interference pattern of the electrons confined in the wedge, and have shown that fundamental predictions of the quantum mechanics in the nanometer regime can be verified to atomic precision. Today the phenomenon of Fizeau fringes is widely used to inspect the quality of modern optics. We believe that imaging electron fringes on thin films as presented here could be developed into a new technique for characterizing buried interfaces in modern material research.

[1] M. Born and E. Wolf, *Principles of Optics* (Pergamon Press Inc., New York, 1980).

[2] A. Tonomura *et al.,* Phys. Rev. Lett. **54**, 60 (1985).

[3] R. C. Jaklevic *et al.,* Phys. Rev. Lett. **26**, 88 (1971).

[4] R. S. Becker, J. A. Golovchenko, and B. S. Swartzentruber, Phys. Rev. Lett. **55**, 987 (1985).

[5] G. Binning *et al.,* Phys. Rev. Lett. **55**, 991 (1985).

[6] M. F. Crommie, C. P. Lutz, and D. M. Eigler, Nature (London) **363**, 524 (1993).

[7] Y. Hasegawa and Ph. Avouris, Phys. Rev. Lett. **71**, 1071 (1993).

[8] M. F. Crommie, C. P. Lutz, and D. M. Eigler, Science **262**, 218 (1993).

[9] M. Jalochowski and E. Bauer, J. Appl. Phys. **63**, 4502 (1988).

[10] H. H. Weitering, D. R. Heslinga, and T. Hibma, Phys. Rev. B **45**, 5991 (1992).

[11] K. Horn *et al.,* Phys. Rev. B **30**, 1711 (1984).

[12] N. W. Ashcroft and N. D. Mermin, *Solid State Physics* (Saunders College, Philadelphia, 1976).

[13] J. R. Anderson and A. V. Gold, Phys. Rev. **139**, A1459 (1965).